Aqueous suspension processing of multicomponent submicronic Y-TZP/Al_2O_3/SiC particles for suspension plasma spraying

V. Carnicer[1], C. Alcazar[2], E. Sánchez[1], R. Moreno[2]

[1] Instituto de Tecnología Cerámica (ITC), Universitat Jaume I, 12006, Castellón, Spain

[2] Instituto de Cerámica y Vidrio (ICV), Consejo Superior de Investigaciones Científicas (CSIC), Universidad Autónoma de Madrid, 28049, Madrid, Spain

Corresponding author at Instituto de Cerámica y Vidrio, E-mail address: rmoreno@icv.csic.es (R. Moreno)

Kelsen 5, 28049 Madrid; tel: +34 917355840

Abstract

In order to obtain thermal barrier coatings by Suspension Plasma Spraying (SPS) process with potential new self-healing ability multicomponent submicronic Y-TZP/Al_2O_3/SiC suspensions were prepared. For this purpose, concentrated aqueous suspensions of individual components as well as the multicomponent mixture were studied and characterised in terms of colloidal stability and rheological behaviour to determine the best conditions for processing and preparation of the coatings. In the study, different dispersant contents and sonication times were tested. Subsequently, low concentrated suspensions were prepared to obtain preliminary thermal barrier coatings with the optimised feedstock. Thus, ceramic coatings were deposited by SPS and then characterised in order to assess the microstructure and phase distribution, in particular, the degree of preservation of the sealing agent, SiC, in the final coating as a previous indicator of its self-healing ability.

1. Introduction

In the last decades, different researchers have developed and studied ceramic coatings with the double purpose of improving the protection and thermal insulation and reducing the surface temperature of the metal components of gas turbine engines, such as rotators, blades... to operate at inlet higher temperatures, increasing the efficiency of the process and the lifetime of these components [1–4]. These materials are called thermal barrier coatings (referred as TBCs). TBCs are composed of refractory ceramic oxides, including alumina, titania, magnesia and their mixtures; however, yttria-doped tetragonal polycrystalline zirconia (Y-TZP) represents the state-of-the-art material as a consequence of its excellent properties at high temperatures compared to metals, such as

low thermal conductivity, low probability of phase transformations at operating temperature, chemical inertness and high melting point, superior to metals or super alloys, among others [5]. Although there are different coating techniques to produce TBCs, atmospheric plasma spraying (APS) is widely used due to its economic and technical feasibility at an industrial scale.

Nowadays, turbines need to operate at higher gas temperatures to improve the engine efficiency; nevertheless these new conditions produce an additional thermal stress and increase the probability of mechanical failure, which causes the appearance and growth of cracks and laminations [2,6]. In the literature, several researchers have proposed to develop a new generation of TBCs with self-healing ability, which will withstand the new working conditions of the turbines and prolong their lifetime [6–11]. SiC is reported as the most efficient ceramic self-healing material, although other metals and alloys are being investigated [6,9,12]. However, self-healing functionality in a TBC has barely started to be developed and, one of the specific challenges is that silicon carbide cannot be easily deposited by plasma spray because it oxidises in the torch before melting [12,13]. The sealing ability (such as in silicon carbide) consists in full filling the cracks originated in the coating, which are produced by the fatigue work of extreme temperatures and aggressive hot gases, during the service time. The self-healing process develops by growing the volume of self-healing particles when the oxygen in the air along with the high environmental temperature goes through the crack, giving rise to the oxidation of self-healing particles located on the edge of the crack [6,8]. Nevertheless, the effectivity of sealing ability is based on the amount and size of non-oxidised particles of the self-healing material found in the coating. .

Literature reports different strategies aiming to preserve the nature of the sealing agent in the final coating obtained by a thermal spray process. Thus, one strategy

employs eutectic mixtures whose melting point is lower than the oxidation temperature of SiC [14,15]. Another sealing mechanism resides in encapsulating the sealing agent (core-shell) by metal compounds, to produce a selective oxidation of the metal elements which prevents the sealing agent from further oxidation [10,16]. Other strategies focus on the development of reducing atmospheres surrounding the sealing particle during the thermal spray process [17].

More recently, some papers have reported the use of the Suspension Plasma Spray (SPS) technique to obtain coatings containing SiC particles [18]. SPS is an emerging thermal spray process in which the powder feedstock is replaced by a suspension feedstock. An important benefit of SPS process is the possibility of spraying very fine, poor flowability powders [3,19–23]. Moreover, the SPS technique would be very favourable to avoid undesirable oxidation of the sealing material because a lot of the plasma energy is destined to solvent (water) evaporation. However, limiting energy during plasma deposition can compromise coating microstructure and adherence since the particles may not melt as much as required [3,19,21]. For this reason, the optimisation of solid content and stability of SPS feedstock containing SiC particles is necessary to obtain coatings in which the amount of SiC particles can be maximised.

This paper reports the first part of an ambitious research based on a mixed strategy which has been chosen to avoid the oxidation of SiC (self-healing agent). On the one hand, SPS technique will be used for the thermal deposition avoiding the contact of SiC particles with an excessively energetic plasma plume. On the other hand, a third component (Al_2O_3) will be added to the Y-TZP matrix in order to enable the formation of a eutectic phase which can favour the protection of SiC particles against oxidation during plasma deposition. Therefore, the great challenge of this first part of the research addresses the preparation and stabilisation of multicomponent aqueous

suspensions of submicronic particles of Y-TZP/Al_2O_3/SiC (referred as SAZ). The literature on the preparation and stabilisation of each of these oxides or their combinations is abundant [22,24–27]. There is also previous research on the preparation of highly concentrated, aqueous suspensions of SiC submicronic particles [28,29]. But the combination of the three ingredients as feedstock for SPS deposition has not been reported to the best of our knowledge. The main purpose is to demonstrate the feasibility of using this formulation to prepare concentrated suspensions to produce homogeneous, self-healing coatings by SPS. For so doing, the stability and rheological behaviour of this 3-component SPS feedstock is firstly studied. Later, a stable, selected feedstock is deposited by SPS and the corresponding coating is characterised in terms of microstructure and crystalline phase distribution.

2. Experimental

2.1. Suspension preparation and characterisation

As starting raw materials, the following commercially available powders were used: 1) α-alumina (CT3000SG, Almatis, Germany), with an average particle size of 0.5 μm and a specific surface area of ~8 m^2/g; tetragonal zirconia polycrystals doped with 3 mol% Y_2O_3 (TZ-3YS, Tosoh, Japan), with an average particle size of 0.4 μm and a surface area of 6.8 m^2/g; and α-SiC (UF-15, Hermann C. Starck, Germany), with an average particle size of 0.6 μm and surface area of 15 m^2/g. The three powders are labelled as A, Z, and S in the following sections. The two oxides were mixed together in such concentrations as to produce after sintering the eutectic composition, i.e. with a relative volume concentration of zirconia/alumina of 50.8/49.2 (that means a weight ratio of 59.6/40.4). The main characteristics of these three powders are shown in Table 1.

Table 1. Characteristics of commercial powders employed in this research.

Characteristics	**Y-TZP**	**Al_2O_3**	**SiC**
Particle size / D_{10} (µm)	0.1	0.3	0.2
Particle size / D_{50} (µm)	0.4	0.5	0.6
Particle size / D_{90} (µm)	1.4	2.0	1.4
Specific surface area (m^2)	6.8	8.0	15
Density (g/cm^3)	6.05	3.97	3.21

Particle size distributions were measured using the laser diffraction technique (LD; Mastersizer S, Malvern, UK) and the morphology of the as-received powders was observed by field-emission gun environmental scanning electron microscopy (FEG-ESEM; Quanta 200 FEG, FEI Company, USA). The crystalline phases were identified by X-ray diffraction (XRD; Advance diffractometer, Bruker Theta-Theta, Germany). In the case of zirconia, the Garvie's approach was used to calculate the relative ratio of tetragonal phase (density = 6.07 g/cm^3, ASTM 83-113) and monoclinic phase (density = 5.82 g/cm^3, ASTM 37-1484), which was found to be 68/32.

Zeta potential measurements were performed using the laser Doppler principle combined with non-invasive back-scattering (Zetasizer Nano-ZS, Malvern, UK). Zeta potentials were firstly measured as a function of pH and secondly as a function of polyelectrolytes. According to previous results concerning the stabilization of aqueous suspensions of the three types of powders used herein an ammonium salt of polyacrylic acid (PAA; Duramax TM D-3005, Rohm & Haas, USA, with 35 wt% active matter) was selected as a deflocculant for both oxides [24,30,31] and a synthetic polyelectrolyte (PKV, Produkt KV5088, Zschimmer-Schwarz, Germany) with unknown composition (but that it is thought to be of polycarboxylic nature), which has demonstrated its suitability for the dispersion of non-oxide ceramics, such as SiC powder [29]. In order

to perform the measurements, diluted suspensions of every powder were prepared to a concentration of 0.01 g/L using KCl 0.01 M as inert electrolyte and adjusting the pH values with HCl and KOH 1M solutions. A pH-meter (Titrino DMS 716, Metrohm, Switzerland) was used for such adjustments. These diluted suspensions were prepared using a sonication probe (UP 400S, Dr Hielscher GmbH, Germany) to avoid agglomerations which can interfere in the analysis. Moreover, suspensions were cooled in an ice-water bath during sonication to avoid excessive heating.

With the aim to optimise the preparation and stabilisation conditions to achieve high stability, concentrated suspensions of every powder were prepared in water to high solids loading of 30 vol.%. Suspensions were always prepared by adding slowly the powder to the water containing the required amount of deflocculant while maintaining the mixture in continuous mechanical agitation with the helix. This high solid loading was used with the purpose of unequivocally detect the differences in viscosity to choose the best rheological conditions. Measurements were performed for different deflocculant contents (from 0.1 to 1.0 wt%) according to a sequential procedure in which the suspension was subjected to sonication for periods of 1 min with intervals of 15 min in which the suspensions were maintained under mechanical agitation. After every sonication treatment applied the rheological behaviour was measured and sonication steps were induced until the viscosity started to increase.

Once optimised the rheological behaviour of the concentrated suspensions, the optimum conditions in terms of deflocculant content and sonication time were used for the preparation of suspensions with lower solids contents, i.e., 10 vol.%. Once studied the behaviour of each material independently mixtures of the two oxides were prepared using a two-step process in which zirconia was added to the total water containing the deflocculant required for its dispersion and in a second step the alumina powder was

incorporated after adding the deflocculant required for its dispersion. Similarly, suspensions with SiC were prepared following this sequence with the final addition of SiC after the incorporation of the deflocculant PKV. The contents of SiC in the final formulation were 6 and 12 wt%. The rheological behaviour of these suspensions was determined using a rheometer (Haake RS50; Thermo, Karlsruhe, Germany) operating at the controlled shear rate by loading the shear rate from 0 to 1000 s^{-1} in 5 min, maintaining at 1000 s^{-1} for 1 min and uploading from 1000 to 0 s^{-1} in 5 min. The measurements were performed at 25°C using a double-cone and plate system with a cone angle of 2°, equipped with a solvent trap to avoid evaporation.

2.2. Coating preparation and characterization

The multicomponent suspensions (SAZ) with a solids content of 10 vol.% were sprayed with SPS technique using an external radial injection monocathode torch (F4-MB, Sulzer Metco, Switzerland) with a 6 mm nozzle, coupled to a six-axis robot (IRB 1400, ABB, Switzerland). The suspensions were injected into the torch using a pneumatic feed system formed by two pressurised containers which force the suspension through the orifice of the injector. Besides, a filter with a mesh of 75 μm was placed before the injector to avoid clogging by agglomerates. This system has been set out in previous research [25,32]. AISI 304 stainless steel disks, with a diameter of 25 mm and 10 mm of thickness, were employed as substrates. Before coatings deposition, the specimens were grit blasted with black corundum, with a particle size distribution ranging from 0.17 to 0.6 mm, and cleaned with ethanol. In addition, the adhesion of the final coatings on the metal substrate was also favoured by means of a commercial bond coat *"Amdry 997"*, whose composition is shown in Table 2. The bond coat was deposited by atmospheric plasma spraying (APS) from commercial powder feedstock

with a particle size distribution between 5 – 38 µm. Later, the samples were preheated at 300°C to further improve the adhesion of the coating.

The spray conditions are detailed in Table 3. These conditions were chosen according to the reviewed literature as well as from previous experience by the research group.

Table 2. The composition of bond coat "Amdry 997".

Element	Ni	Al	Co	Cr	Ta	Y
Composition (in wt%)	43.9	8.5	23	20	4	0.6

Table 3. Plasma spray conditions employed for bond and top coats deposition.

Parameters	Bond coat (APS)	SAZ coat (SPS)
Ar flow rate (slpm [1])	65	37
H_2 flow rate (slpm [1])	8	8
Intensity (A)	650	700
Stand-off distance (m)·10^3	145	40
Surface speed (m·s^{-1})	1	1.25
Number of passages	1	5
Pre-heating (K)	150	300
Injector diameter (m)·10^4	15	1.50
Powder feed rate (kg·s^{-1})	0.04	-
Specimen holder velocity (m·s^{-1})	-	0.72
SAZ solid content (vol.%)	-	10
Suspension feed rate (m^3·s^{-1}) ·10^7	-	4.86

[1] Slpm: standard litre per minute.

The coatings were prepared metallographically (mounted in resin, cutted and polished) and the polished faces were analysed using FEG-ESEM technique. X-ray diffraction was employed to identify crystalline phases in the coatings using a Cu Kα radiation.

On the other hand, coating thickness was measured by optical microscopy and the porosity was assessed by image analysis (Micro Image software, Olympus Optical

Co GmBH, Germany, Europe) from FEG-ESEM micrographs taken at 2000x magnification. For each coating, a total of 20 FEG-ESEM micrographs were analysed and the final porosity value was averaged.

3. Results and discussion

3.1 Powders of the multicomponent suspension feedstock

The particle size distribution of the as-received commercial powders employed to prepare the different suspensions are shown in Table 1 and Fig. 1. As expected all powders exhibit their submicron-sized character but the distribution of alumina and silicon carbide is narrower, in comparison with that of zirconia, although zirconia distribution shifts left to finer particle size. In the SEM micrographs of the powders at different magnifications (Fig. 2), it can be observed that zirconia (pictures a and d) and alumina (pictures b and e) present similar morphology with round edges whereas Al_2O_3 sample shows wider particle size distribution as well as the presence of some non-spherical agglomerates probably formed by humidity cohesion. In addition, Y-TZP powder particles are quite agglomerated forming sort of small spheres. On the other hand, SiC sample is characterised by particles with angular edges which are quite common in SiC powders obtained my mechanical grinding.

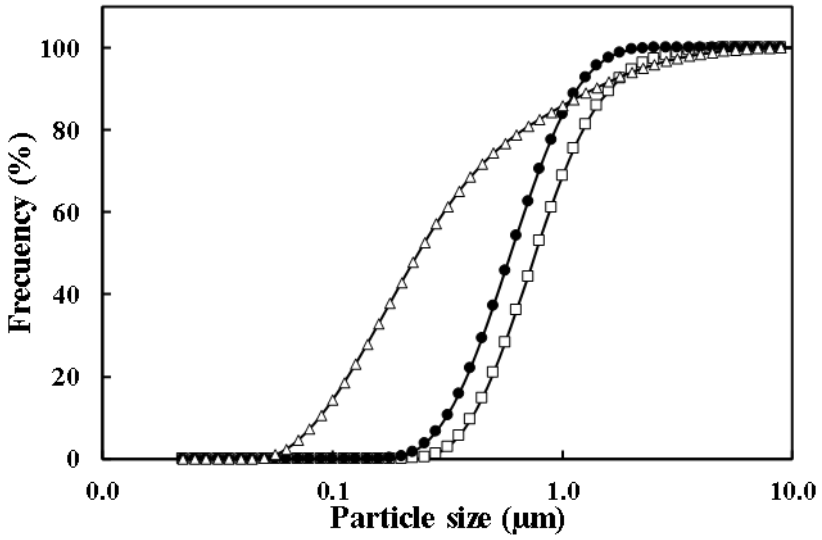

Fig. 1 Particle size distribution of the different powders. □: Al_2O_3, ●: SiC, △: Y-TZP.

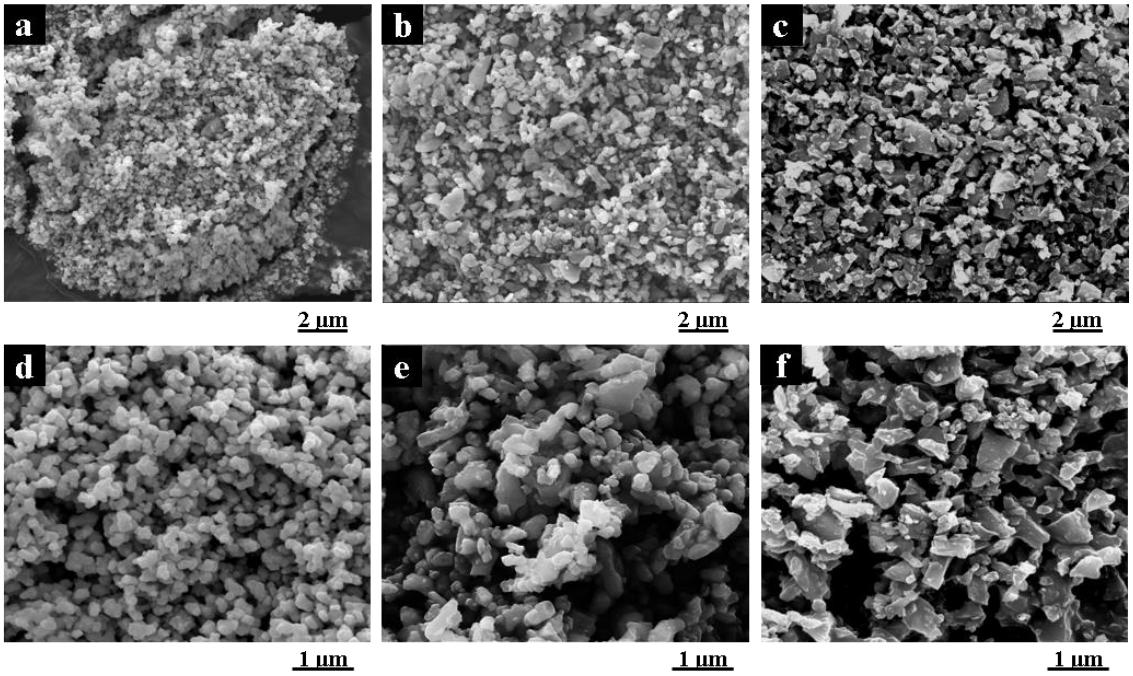

Fig. 2 Micrographs showing the morphology as the as-received powders as observed by FEG-ESEM for Y-TZP (a,d), Al_2O_3 (b,e), and SiC (c,f) powders at two magnification, 20000x (a,b,c) and 50000x (d,e,f).

3.2 Study of the colloidal and rheological behaviour of the suspensions

To evaluate the colloidal stability of the different powders in water, zeta potential measurements as a function of pH were performed without polyelectrolyte and

with different additions of polyelectrolytes, PAA for the oxides and PKV for SiC (Fig. 3).

Fig. 3a shows the variation of zeta potential as a function of pH for alumina suspensions containing different concentrations of deflocculant. It can be seen that the isoelectric point occurs at pH~8 for the suspension without polyelectrolyte in good agreement with other values reported in the literature [26]. The zeta potential reaches a value large enough to assure stability at pH near 10, which are quite aggressive conditions. In the acidic part of the curve, the zeta potential values are lower than 20 mV, which is considered too low to provide stability. Thus, the addition of polyelectrolyte is needed to improve the dispersion. The complete curves as a function of pH were determined for suspensions containing deflocculant percentages ranging from 0.1 to 1.0 wt%. As expected, the isoelectric point shifts down to lower pHs as the deflocculant content increases, with isoelectric points (referred as iep) moving toward pHs of 4.8, 3.9, 3.1, 2.8 and 2.8 for PAA contents of 0.1, 0.2, 0.5, 0.8, and 1.0 wt%. The gap after every addition reduces and the iep does not move anymore after the addition of 0.8 wt%, thus suggesting that further additions do not adsorb onto the particles surfaces. However, although there is a slight variation for higher contents, the addition of 0.2 wt% PAA shifts strongly the iep and provides high values of zeta potential at neutral pH (-52 mV at pH 6), enough to assure stabilisation.

The variation of zeta potential versus pH for zirconia suspensions is plotted in Fig. 3b. The isoelectric point occurs at pH~6, in good agreement with previously reported values [30–32]. The addition of 0.2 wt% PAA shifts down the iep to pH 3 and provides large values of zeta potential at neutral pH (-60 mV at pH 6). The addition of 0.5 wt% PAA produces a very small shift of the iep, thus suggesting that 0.2 wt% is the

right concentration to achieve full coverage and good dispersion with least amount of PAA.

The stabilisation of SiC was studied in previous works by Candelario et al. [28,29] showing an iep of pH~3.8. In this paper, it was demonstrated that the zeta potential did not significantly change with the addition of the PKV polyelectrolyte whereas its addition was essential for the preparation of concentrated suspensions due to the steric effect contribution to the stabilisation that promoted a great reduction in viscosity. In Fig. 3c the variation of zeta potential as a function of pH with an addition of 1.5 wt% is plotted, showing the similarity with the suspension without PKV shown in reference [28].

From all these data, it can be concluded that concentrations of 0.2-0.3 wt% PAA are enough for the stabilisation of the oxides while a content of 1.5 wt% was used for SiC-based on previous results.

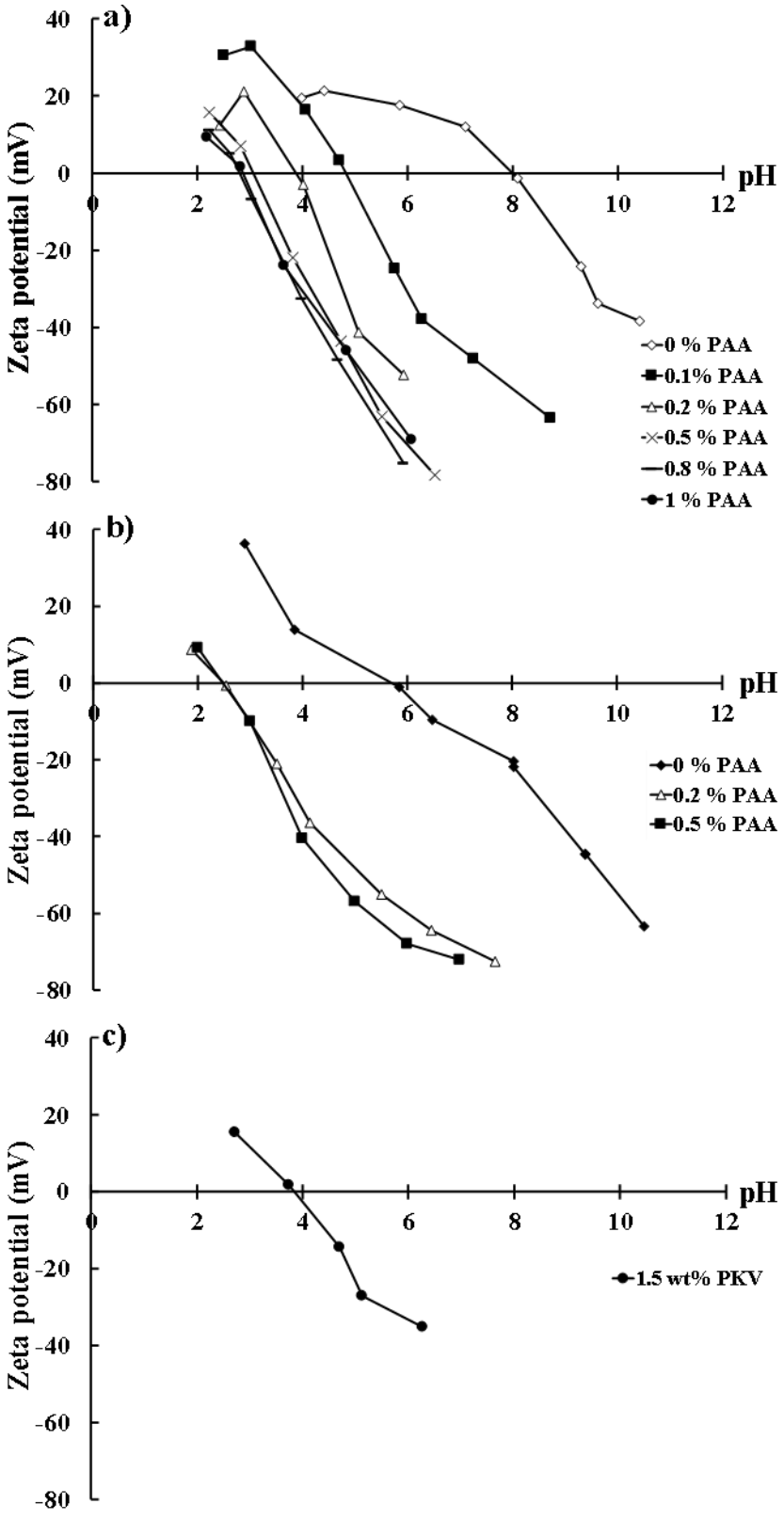

Fig. 3 Evolution of zeta potential of suspensions of the different starting powders as a function of pH for different deflocculant concentrations: Influence of PAA on zeta potential of alumina (a) and Y-TZP (b) and influence of PKV on SiC zeta potential.

Since the suspensions to be used for SPS can present relatively low solids content due to the viscosity limitations imposed by the suspension injection system [3,33], SPS suspension viscosity can be very low and subjected to a large measurement error. In order to optimise the rheological behaviour, it was preferable to prepare concentrated suspensions with 30 vol.% solids in order to unequivocally detect the best dispersing conditions in terms of deflocculant content and sonication time. Fig. 4 shows the flow curves of 30 vol.% alumina suspensions with different PAA contents and sonication times. Suspensions homogenised only with helices present always higher viscosity and a broad thixotropic cycle that reveals an evident lack of dispersion so that sonication is absolutely necessary in order to achieve well-dispersed suspensions. For the sake of simplicity, the flow curves of suspensions prepared without sonication are not presented in the plots. Sonicated suspensions exhibit a Newtonian behaviour with very low viscosity values and no thixotropy at all. The minimum viscosities are obtained for deflocculant contents of 0.2-0.3 wt% with 1-2 min sonication. In order to allow an easy comparison, the viscosity values at the maximum shear rate (1000 s^{-1}) of all alumina suspensions with different PAA contents as a function of sonication time are plotted in Fig. 5.

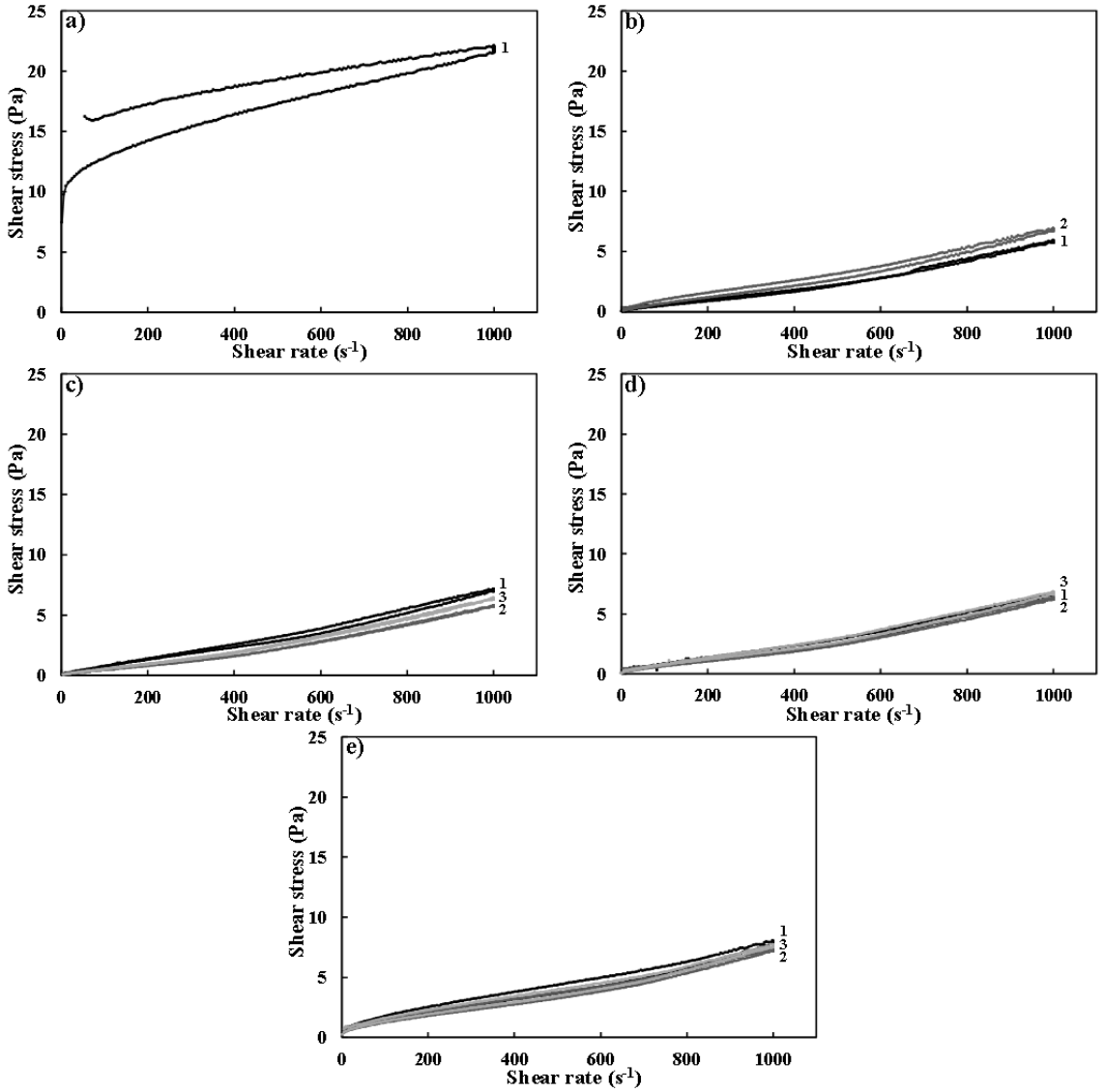

Fig. 4 Flow curves of the concentrated suspensions of alumina prepared at 30 vol.% solids with different sonication times and dispersed with a) 0.1, b) 0.2, c) 0.3, d) 0.5 and e) 0.8 wt% of PAA. The number at the right of each curve denotes the sonication time in minutes.

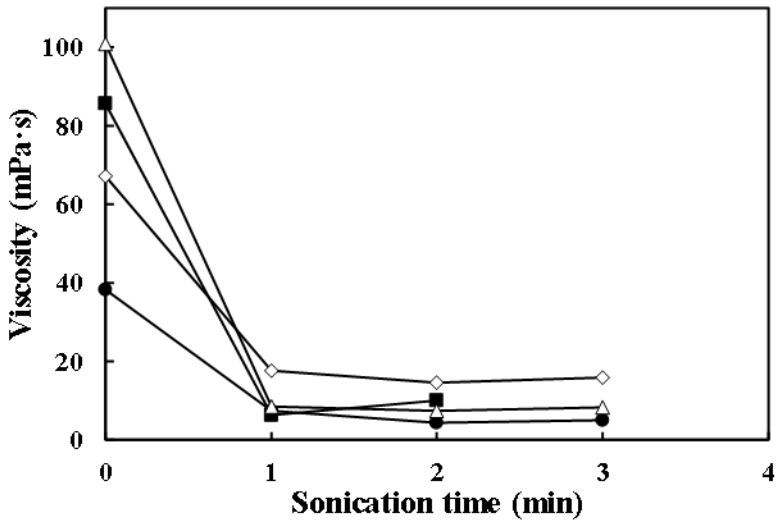

Fig. 5 Influence of sonication time on the viscosity of alumina suspensions with different contents of PAA: 0.2 (■), 0.3 (●), 0.5 (△), and 0.8 (◊) wt% PAA.

Following the same procedure as for alumina, suspensions of zirconia were prepared to solids loadings of 30 vol.% in order to optimise the dispersions on the basis of the deflocculant content and sonication time. The resulting flow curves are shown in Fig. 6. Once again, the preparation with just mechanical agitation leads to high viscosity and very broad thixotropic cycles that demonstrate an evident lack of homogeneity. A difference between these flow curves and those of alumina is that the former present a thixotropic cycle although the thixotropic areas are rather small. Table 4 shows this comparison. A summary of the viscosities as a function of the sonication time and deflocculant content is presented in Fig. 7, in which it can be seen that the viscosity largely decreases for 1 min sonication and decreases very slowly with longer sonication times. It is also clearly observed that the minimum viscosity is reached with 0.2 wt% PAA and 1 min of sonication time because the values of viscosity and thixotropy are lower for the minimum quantity of deflocculant and sonication time.

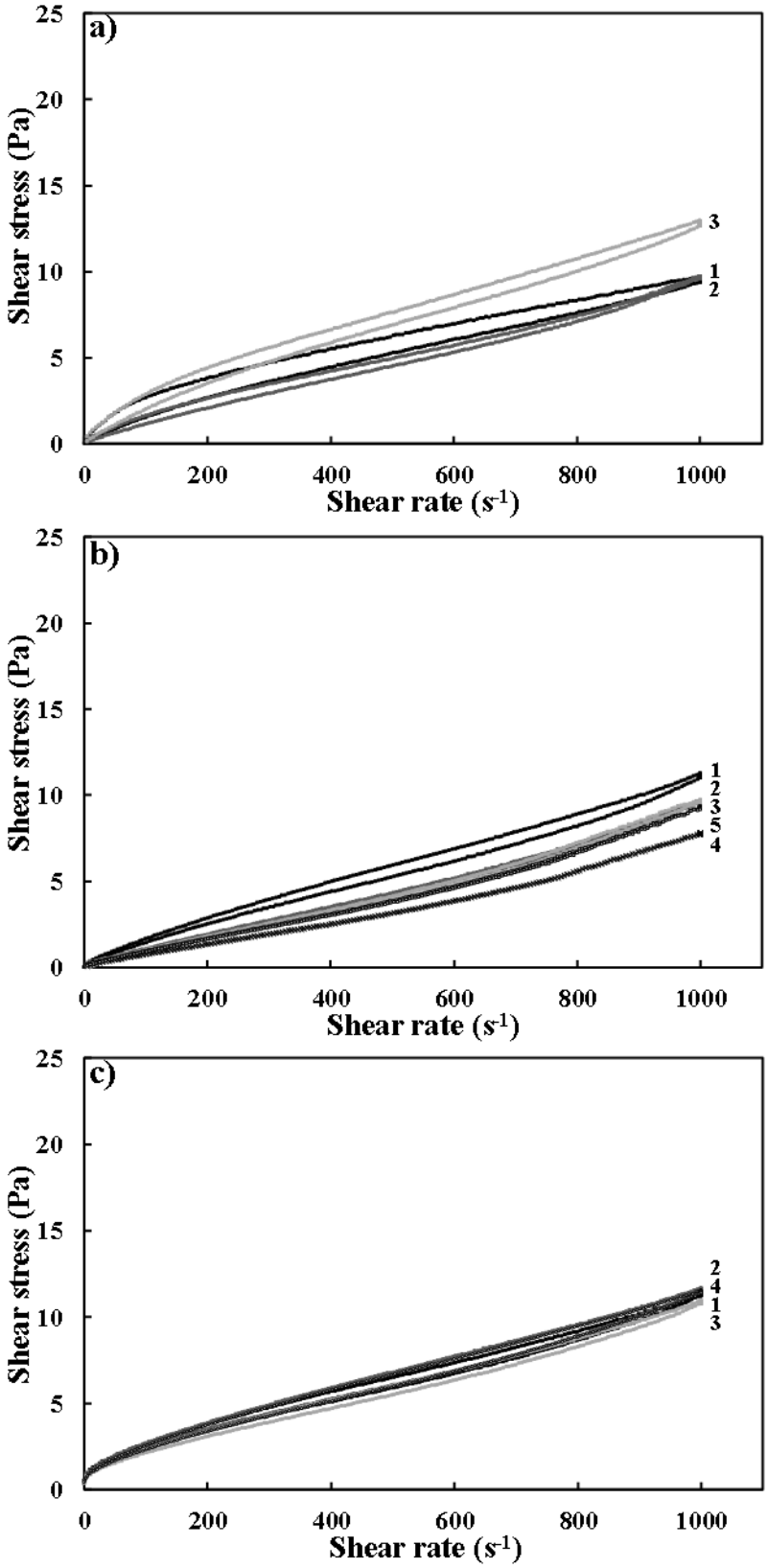

Fig. 6 Flow curves of the concentrated suspensions of Y-TZP prepared to 30 vol.% solid with different sonication times and dispersed with a) 0.1, b) 0.2 and c) 0.3 wt% of PAA. The number at the right of each curve denotes the sonication time in minutes.

Table 4. Values of thixotropy and viscosity (measured at 1000 s^{-1} shear rate in uploading step) of the concentrated suspensions (30 vol.%) for alumina and zirconia with 0.2 and 0.3 wt% PAA for 1 and 2 min sonication time, represented in Fig. 4 and Fig. 6.

Suspension	PAA content (wt%)	Sonication time (min)	Viscosity (mPa·s)	Thixotropy ($Pa \cdot s^{-1}$)
Al_2O_3	0.2	1	5.9	342
		2	6.8	840
	0.3	1	7.2	490
		2	5.7	136
Y-TZP	0.2	1	11.2	992
		2	9.6	326
	0.3	1	11.4	866
		2	11.6	1040

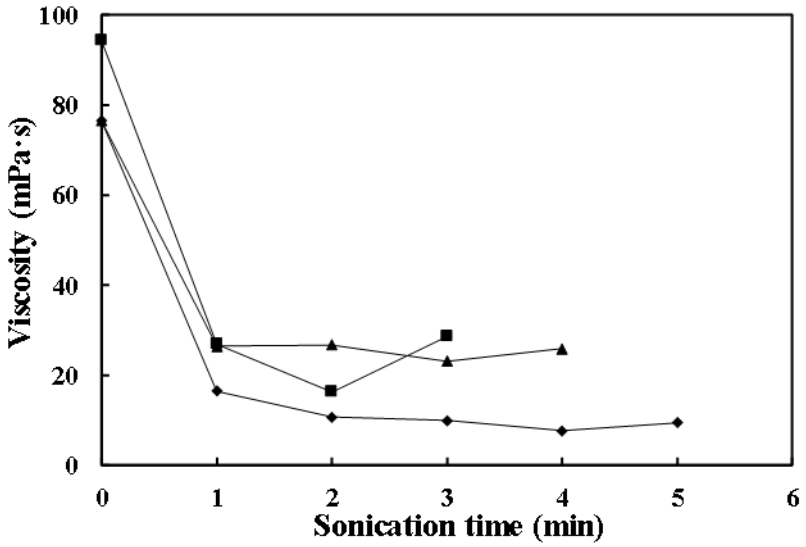

Fig. 7 Influence of sonication time on the viscosity of Y-TZP suspensions with different contents of PAA: 0.1 (■), 0.2 (♦) and 0.3 (▲) wt% PAA.

Finally, for the dispersion of SiC, a constant polyelectrolyte PKV content of 1.5 wt% was selected, as this was reported to be the optimum content in the works of Candelario et al. [28,29].

After selecting the best-dispersing conditions for these concentrated suspension new suspensions were prepared to a solid loading of 10 vol.%. To confirm the adequacy of the selected conditions the flow curves of the diluted suspensions of the single component suspensions, the eutectic mixture (alumina-zircona) and the final SPS

feedstock mixtures with 6 and 12 wt% SiC were measured. In all cases, fresh suspensions were prepared with mechanical agitation and subsequently sonicated. Fig. 8 shows the flow curves with and without sonication for suspensions of A, Z, and SiC prepared with 0.2 wt% PAA for every oxide and 1.5 wt% PKV for the carbide. As expected, sonication reduces the viscosity and makes the thixotropic cycle to completely disappear. Therefore, the curves appear to be slightly shear thickening but this is an apparent effect related to the possible slippage at the surface of the measuring systems and is always observed in diluted suspensions and sol-gel solutions with extremely low viscosity [34]. The viscosities are extremely low due to the low solids content, nearly the error limit of the rheometer, and no differences can be seen among them, which explains why the optimisation was performed with higher solids content. In Fig. 9 it can be seen that the addition of different silicon carbide proportions to suspension (6 and 12 wt%) do not modify the flow curves and they overlap. Therefore, it is determined that the suspensions are correctly stabilised because the rheological behaviour of all is identical, i.e, they have a low viscosity and no thixotropy, as can be seen in Table 5.

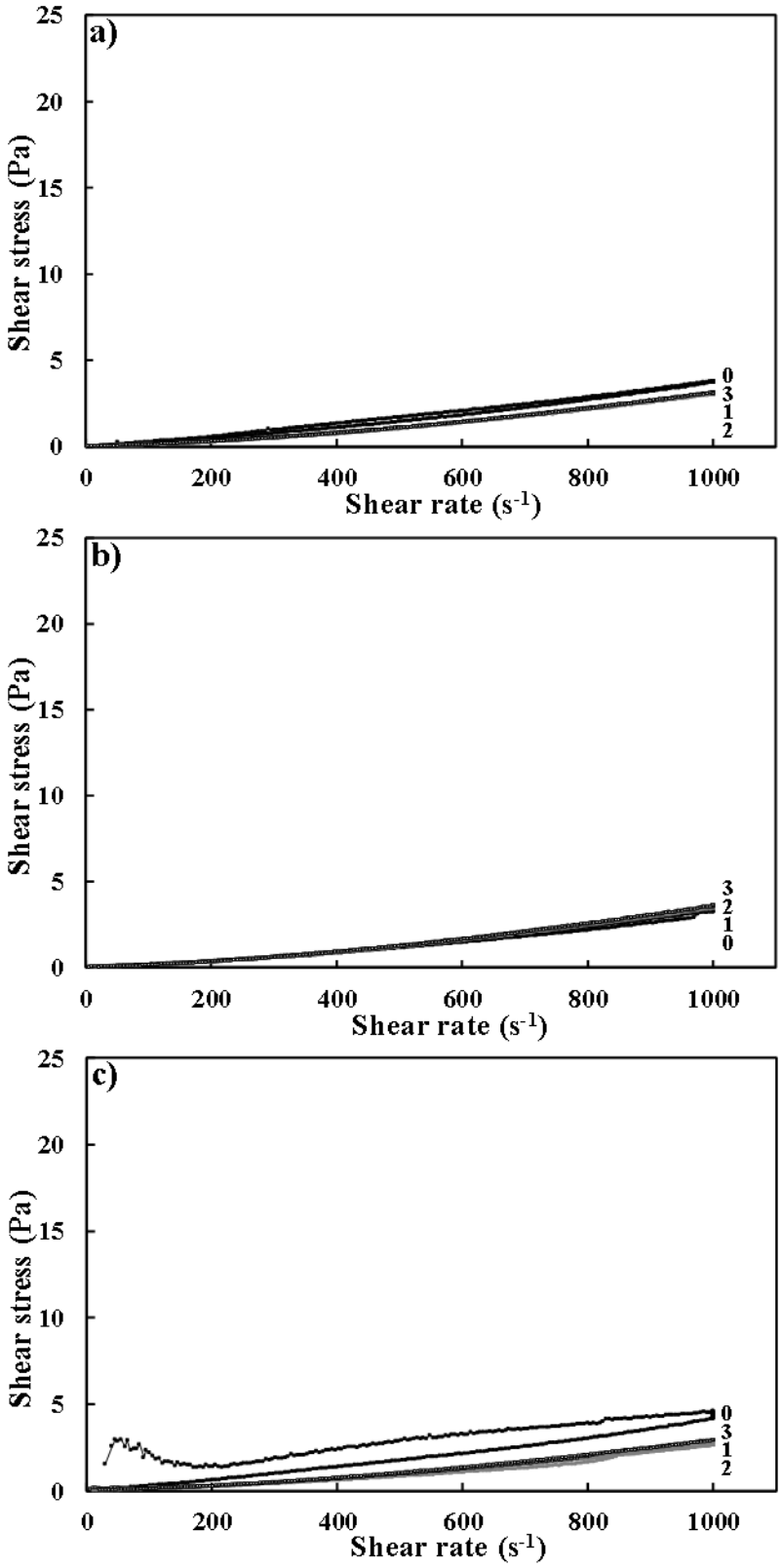

Fig. 8 Flow curves of the diluted suspensions prepared at 10 vol.% solid with different sonication times. a) Suspension of alumina and dispersed with 0.2 wt% of PAA, b) Suspension of yttria stabilised zirconia and dispersed with 0.2 wt% of PAA and c) Suspension of silicon carbide and dispersed with 1.5 wt% of PKV. The number at the right of each curve denotes the sonication time in minutes.

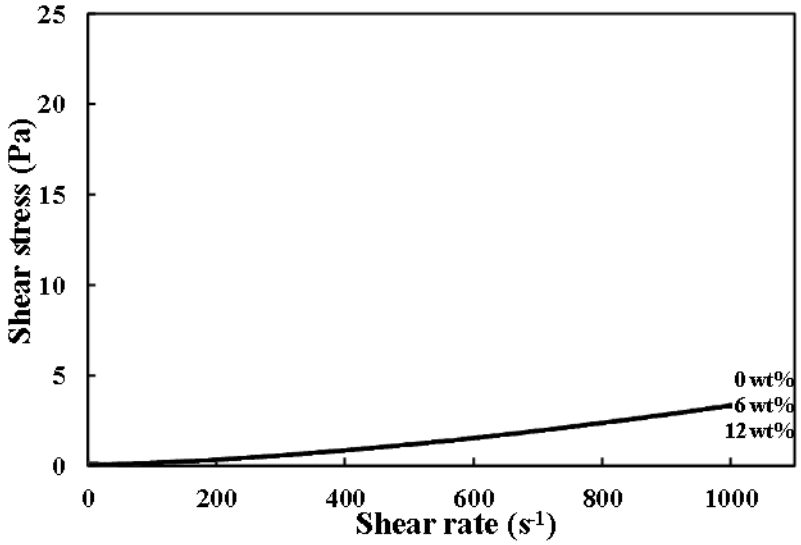

Fig. 9 Flow curves of the diluted suspensions of multicomponent (Al_2O_3, Y-TZP and SiC) prepared at 10 vol.% solid with two minutes of sonication time for different silicon carbide content.

Table 5. Values of thixotropy and viscosity (measured at 1000 s^{-1} shear rate in uploading step) of the diluted suspensions (10 vol.%) of alumina and zirconia with and without SiC sonicated for 1 min. The contents of deflocculant were 0.2 wt% PAA for the oxides and 1.5 wt% PKV for SiC.

Condition	Viscosity (mPa·s)	Thixotropy (Pa·s^{-1})
Al_2O_3/Y-TZP	3.3	17
Al_2O_3/Y-TZP/SiC (6wt%)	3.3	39
Al_2O_3/Y-TZP/SiC (12wt%)	3.3	31

3.3 Microstructure of coatings obtained from diluted multicomponent suspension

Once the behaviour of the suspensions was observed and the optimal amounts of deflocculants were determined to stabilise the three components mixtures, two suspension feedstocks were prepared to be deposited by SPS. In this first attempt to obtain multicomponent coatings the feedstocks were prepared at relatively low solid content, i.e 10 vol.% so as to avoid possible problems related to suspension injection [3]. With regard to the self-healing agent, SiC, two concentrations (6 and 12 wt%

referred to total solids) were tested with the aim at better observing the content and distribution of SiC in the final coating matrix. Both coatings were deposited according to the conditions shown in Table 3.

Fig. 10 shows the FEG-ESEM cross-sectional microstructures of the two coatings. As it can be observed, both microstructures show similarity to those reported in the literature for SPS coatings obtained from aqueous suspensions. Hence, the melted particles are homogeneously found in the coating. On the other hand, the typical plasma-deposited splats are not observed in the coatings seeming that on the surface of the coating the base of the columnar structures, or also called cauliflower-like, begins to form [3,9,27,30,31].

Moreover, the two coatings exhibit similar porosities, partially molten areas, and irregular surface and have constant thicknesses, evidencing the scarce influence of the SiC particles content on the coating microstructural homogeneity. The bond layer has a constant thickness of 25 μm for both coatings, while the top coat thickness is about 55-60 μm.

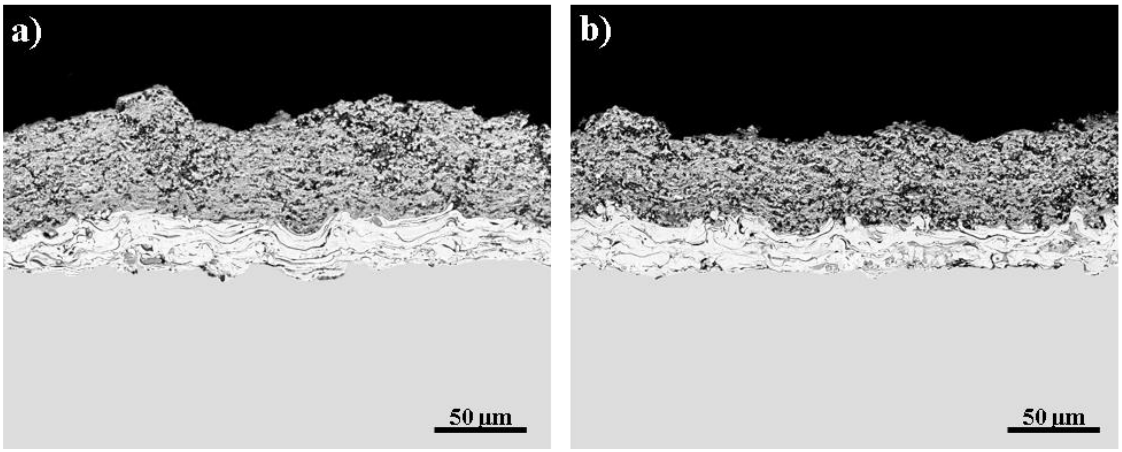

Fig. 10 FEG-ESEM cross-sectional micrographs for coatings obtained with 10 vol.% solid content suspensions at two concentration of SiC: a) 6 and b) 12wt%.

Fig. 11 shows micrographs of these same coatings at higher magnifications, in order to analyse the different coating zones as well as the presence of SiC particles, their

nature and distribution. As observed, both micrographs show the presence of black zones with interconnected pores (marked P in the micrographs) and melted areas of greyish coloration (light grey) characterised by rounded edges (marked LG in the micrographs). This grey-coloured, melted matrix corresponds to the pseudo eutectic mixture of zirconia and alumina [35], which is distributed throughout the coating. Within these melts, it can be distinguished whitish particles or areas (marked W in the micrographs), which correspond to particles with the highest contents of zirconia according to c)-EDX. There are also zones in the matrix with dark grey coloration (marked DG) that correspond to higher contents of alumina, according to d)-EDX. Finally, in both matrices but mainly in the micrograph of figure 11.b, a high presence of isolated particles with high silicon contents can be observed, there particles present an angular or subangular morphology (marked arrows). These particles are assumed to correspond to silicon carbide as deduced by e)-EDX.

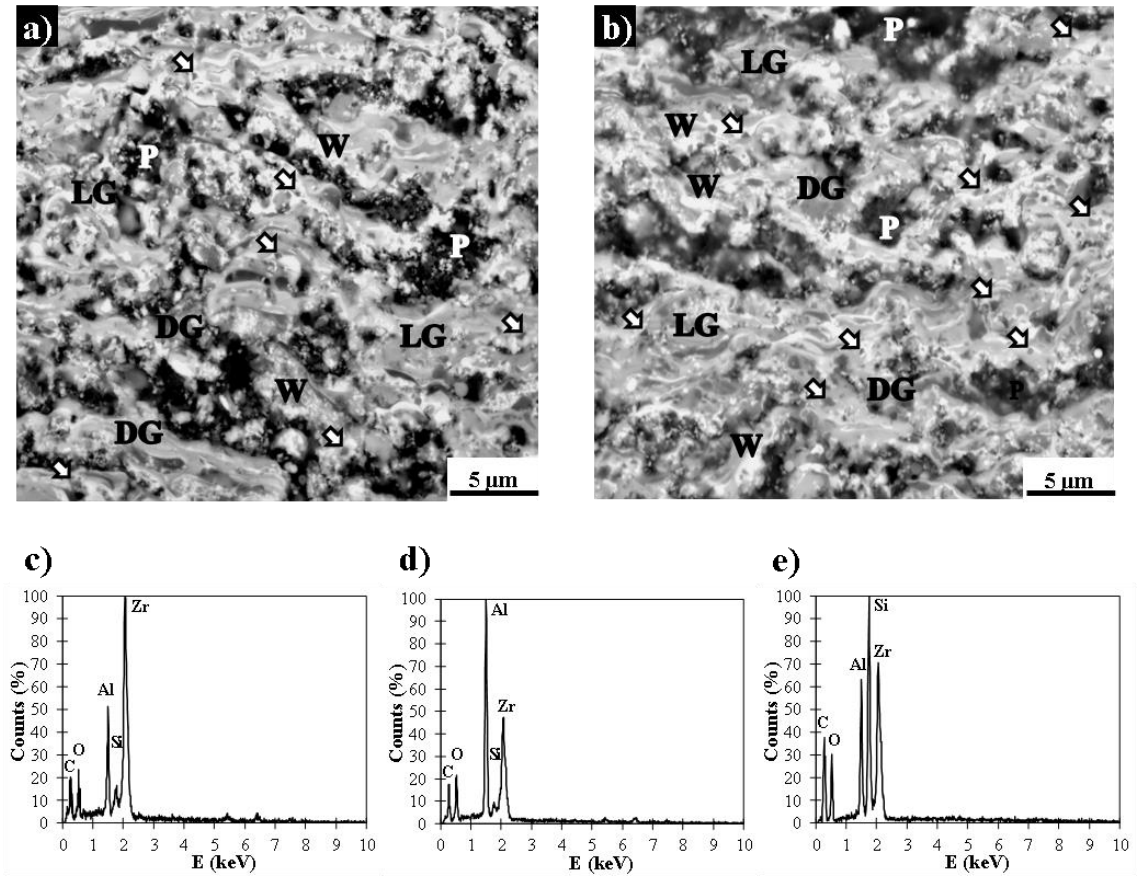

Fig. 11 FEG-ESEM micrographs for coatings obtained from 10 vol.% suspensions at high magnifications, and EDX corresponding to different areas of the coatings. a, b) Coatings obtained with 6 and 12 wt% of silicon carbide respectively, c, d and e) EDX analysis of different areas observed in the matrix of the coatings.

From the above coatings, XRD analysis was performed to determine the crystalline phases present in the coatings and therefore to be able to assess the protective effect of the chosen strategies carried out in this research. Fig. 12 shows the XRD patterns of both coatings. As observed, the two coatings display practically identical XRD patterns, including almost the same zirconia and alumina peaks, however, a small silicon carbide peak can be distinguished, while peaks or phases of silica are not present. The appreciation of this SiC peak is not easy since it is quite overlapped with alumina and zirconia peaks [13,36]. Nevertheless, the SiC peak is a little bit more visible as the SiC content in the coating sample increases (12 wt% against 6 wt%). This finding indicates that, in principle, a significant amount of the initial SiC has not been

either oxidised or decomposed during the plasma deposition. However, this finding should be confirmed by analysing more samples as well as complementary XPS assessment. As a consequence, the addition of alumina to the zirconia matrix together with SPS projection technique seem to be efficient in order to preserve the nature of the SiC particles in the final plasma sprayed coating.

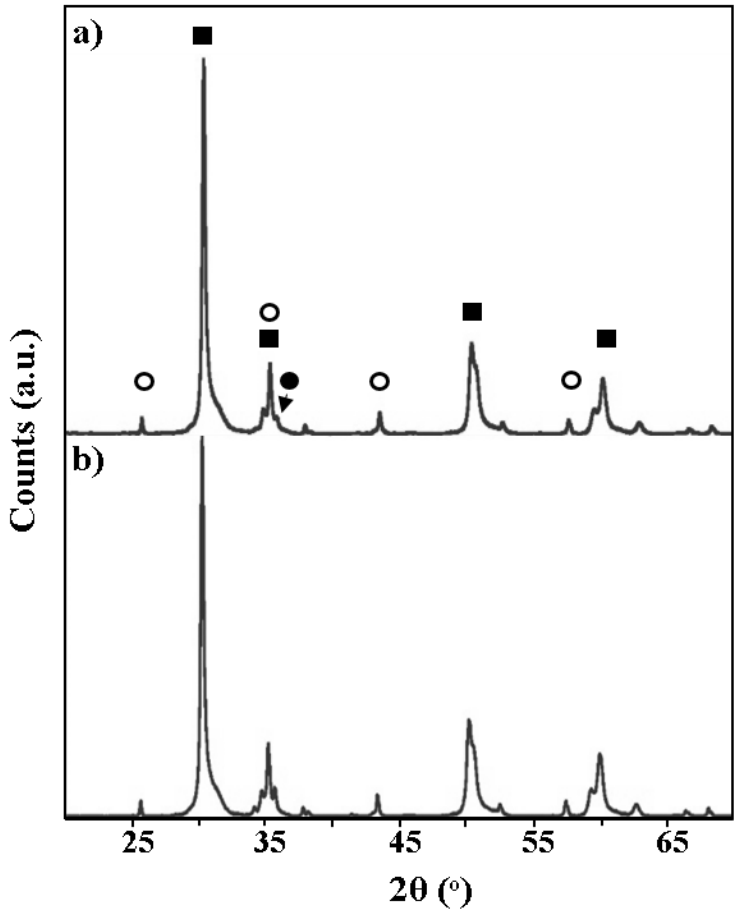

Fig. 12 XRD patterns of the ceramic coatings resulting from the multicomponent suspension SAZ (10 vol.%) with 3 min of sonication. a) Coating with 6 wt% of SiC and b) Coating with 12 wt% of SiC. Bold circle corresponds to the peak of alpha silicon carbide, hollow circle to peaks of alpha alumina, and bold square to peaks of tetragonal Y-TZP.

4. Conclusions

In this work, the combination of two strategies to avoid oxidation of SiC in a zircona-alumina matrix to be used as thermal barrier coating has been addressed. The

multicomponent mixture of zircona-alumina-SiC has been prepared to be deposited by Suspension Plasma Spraying (SPS). Thus, multicomponent aqueous suspensions were prepared from submicron particle size of the three ingredients at two different percentages of SiC particles. Suspensions were stabilised by means of Z-potential and viscosity measurements were carried out to optimise dispersant content and sonication time. High solids content suspensions up to 30 vol.% solids, firstly for the powders separately and then for the multicomponent mixture were prepared in order to unequivocally detect the best dispersing conditions in terms of dispersant content and sonication time. A minimum of viscosity was found for the following conditions: 0.4 wt% of PAA for oxides, 1.5 wt% of PKV for silicon carbide and three minutes of sonication time.

Optimal suspension feedstock containing two different content of SiC were successfully prepared and then deposited by SPS with the purpose to obtain preliminary coatings. The microstructure was characterised in terms of porosity and phase distribution with special focus on the assessment of the presence of the initial SiC particles. Although the silicon carbide particles in the coating were mainly well preserved, the coating displayed high porosity as a consequence of a lack of energy during plasma deposition. Moreover, the thickness of the coatings is, in general, lower than that of the conventional thermal barriers coatings obtained by SPS process. For that purpose, more research is in progress regarding the optimisation of the thermal spray conditions to improve the coating microstructure by enhancing the melting of the matrix particles but simultaneously preserving SiC particles in the same.

The results of this work allow us to conclude that the selected dispersing materials and conditions are adequate to prepare a multicomponent submicron size particle

suspension to be used in the development of thermal barrier coatings with potential self-healing ability by SPS process.

Acknowledgements

This work has been supported by the Spanish Ministry of Economy, Industry and Competitiveness and FEDER Funds under the Grant no. MAT2015-67586-C3-R.

References

[1] D.R. Clarke, M. Oechsner, N.P. Padture, Thermal-barrier coatings for more efficient gas-turbine engines, MRS Bull. 37 (2012) 891–898. doi:10.1557/mrs.2012.232.

[2] R. Gadow, M. Floristán, Future Development of Thermal Spray Coatings: Types, Designs, Manufacture and Applications, Woodhead publishing, 2015. doi:10.1016/B978-0-85709-769-9.00011-7.

[3] A. Guignard, Development of thermal spray processes with liquid feedstocks, Schriften des Forschungszentrums Jülich Reihe Energie & Umwelt / Energy & Environment, Jülich, Germany, 2012. http://www.fz-juelich.de/zb/juwel.

[4] C.U. Hardwicke, Y.C. Lau, Advances in thermal spray coatings for gas turbines and energy generation: A review, J. Therm. Spray Technol. 22 (2013) 564–576. doi:10.1007/s11666-013-9904-0.

[5] X.Q. Cao, R. Vassen, D. Stoever, Ceramic materials for thermal barrier coatings, J. Eur. Ceram. Soc. 24 (2004) 1–10. doi:10.1016/S0955-2219(03)00129-8.

[6] S.K. Ghosh, Self-healing materials : fundamentals, design strategies, and applications, Wiley-VCH, Weinheim, Germany, 2009. doi:10.1002/9783527625376.

[7] D.G. Bekas, K. Tsirka, D. Baltzis, A.S. Paipetis, Self-healing materials: A review

of advances in materials, evaluation, characterization and monitoring techniques, Compos. Part B Eng. 87 (2016) 92–119. doi:10.1016/j.compositesb.2015.09.057.

[8] Z. Derelioglu, S. Turteltaub, S. Van Der Zwaag, W.G. Sloof, Healing Particles in Self-Healing Thermal Barrier Coatings, (n.d.) 578–581.

[9] T. Ouyang, X. Fang, Y. Zhang, D. Liu, Y. Wang, S. Feng, T. Zhou, S. Cai, J. Suo, Enhancement of high temperature oxidation resistance and spallation resistance of SiC-self-healing thermal barrier coatings, Surf. Coatings Technol. 286 (2016) 365–375. doi:10.1016/j.surfcoat.2015.12.054.

[10] F. Nozahic, D. Monceau, C. Estournès, Thermal cycling and reactivity of a MoSi2/ZrO2 composite designed for self-healing thermal barrier coatings, Mater. Des. 94 (2016) 444–448. doi:10.1016/j.matdes.2016.01.054.

[11] R. Das, C. Melchior, K.M. Karumbaiah, Self-healing composites for aerospace applications, Elsevier Ltd, 2016. doi:10.1016/B978-0-08-100037-3.00011-0.

[12] M. Tului, B. Giambi, S. Lionetti, G. Pulci, F. Sarasini, T. Valente, Silicon carbide based plasma sprayed coatings, Surf. Coatings Technol. 207 (2012) 182–189. doi:10.1016/j.surfcoat.2012.06.062.

[13] Z. Károly, C. Bartha, I. Mohai, C. Balázsi, I.E. Sajõ, J. Szépvölgyi, Deposition of silicon carbide and nitride-based coatings by atmospheric plasma spraying, Int. J. Appl. Ceram. Technol. 10 (2013) 72–78. doi:10.1111/j.1744-7402.2011.02748.x.

[14] C. Bartuli, T. Valente, M. Tului, Plasma spray deposition and high temperature characterization of ZrB2 - SiC protective coatings, Surf. Coatings Technol. 155 (2002) 260–273. doi:10.1016/S0257-8972(02)00058-0.

[15] P. Wang, W. Han, X. Zhang, N. Li, G. Zhao, S. Zhou, (ZrB2-SiC)/SiC oxidation protective coatings for graphite materials, Ceram. Int. 41 (2015) 6941–6949. doi:10.1016/j.ceramint.2015.01.149.

[16] Z. Derelioglu, A.L. Carabat, G.M. Song, S. van der Zwaag, W.G. Sloof, On the use of B-alloyed MoSi2 particles as crack healing agents in yttria stabilized zirconia thermal barrier coatings, J. Eur. Ceram. Soc. 35 (2015) 4507–4511. doi:10.1016/j.jeurceramsoc.2015.08.035.

[17] C. Hu, Y. Niu, H. Li, M. Ren, X. Zheng, J. Sun, SiC coatings for carbon/carbon composites fabricated by vacuum plasma spraying technology, J. Therm. Spray Technol. 21 (2012) 16–22. doi:10.1007/s11666-011-9697-y.

[18] F. Mubarok, N. Espallargas, Suspension Plasma Spraying of Sub-micron Silicon Carbide Composite Coatings, J. Therm. Spray Technol. 24 (2015) 817–825. doi:10.1007/s11666-015-0242-2.

[19] A. Joulia, G. Bolelli, E. Gualtieri, L. Lusvarghi, S. Valeri, M. Vardelle, S. Rossignol, A. Vardelle, Comparing the deposition mechanisms in suspension plasma spray (SPS) and solution precursor plasma spray (SPPS) deposition of yttria-stabilised zirconia (YSZ), J. Eur. Ceram. Soc. 34 (2014) 3925–3940. doi:10.1016/j.jeurceramsoc.2014.05.024.

[20] D. Li, J. Feng, H. Zhao, C. Liu, L. Zhang, F. Shao, Y. Zhao, S. Tao, Microstructure formed by suspension plasma spraying: From YSZ splat to coating, Ceram. Int. 43 (2017) 7488–7496. doi:10.1016/j.ceramint.2017.03.027.

[21] W. Fan, Y. Bai, Review of suspension and solution precursor plasma sprayed thermal barrier coatings, Ceram. Int. 42 (2016) 14299–14312. doi:10.1016/j.ceramint.2016.06.063.

[22] B. Bernard, A. Quet, L. Bianchi, A. Joulia, A. Malié, V. Schick, B. Rémy, Thermal insulation properties of YSZ coatings: Suspension Plasma Spraying (SPS) versus Electron Beam Physical Vapor Deposition (EB-PVD) and Atmospheric Plasma Spraying (APS), Surf. Coatings Technol. 318 (2016) 122–

128. doi:10.1016/j.surfcoat.2016.06.010.

[23] L. Pawlowski, Suspension and solution thermal spray coatings, Surf. Coatings Technol. 203 (2009) 2807–2829. doi:10.1016/j.surfcoat.2009.03.005.

[24] D. Waldbillig, O. Kesler, The effect of solids and dispersant loadings on the suspension viscosities and deposition rates of suspension plasma sprayed YSZ coatings, Surf. Coatings Technol. 203 (2009) 2098–2101. doi:10.1016/j.surfcoat.2008.11.027.

[25] E. Bannier, M. Vicent, E. Rayón, R. Benavente, M.D. Salvador, E. Sánchez, Effect of TiO2 addition on the microstructure and nanomechanical properties of Al2O3 Suspension Plasma Sprayed coatings, Appl. Surf. Sci. 316 (2014) 141–146. doi:10.1016/j.apsusc.2014.07.168.

[26] T. Røn, S. Lee, Reduction in friction and wear of alumina surfaces as assisted with surface-adsorbing polymers in aqueous solutions, Wear. 368–369 (2016) 296–303. doi:10.1016/j.wear.2016.09.025.

[27] M. Vicent, E. Bannier, P. Carpio, E. Rayón, R. Benavente, M.D. Salvador, E. Sánchez, Effect of the initial particle size distribution on the properties of suspension plasma sprayed Al2O3-TiO2 coatings, Surf. Coatings Technol. 268 (2015) 209–215. doi:10.1016/j.surfcoat.2014.12.010.

[28] V.M. Candelario, M.I. Nieto, F. Guiberteau, R. Moreno, A.L. Ortiz, Aqueous colloidal processing of SiC with Y3Al5O12 liquid-phase sintering additives, J. Eur. Ceram. Soc. 33 (2013) 1685–1694. doi:10.1016/j.jeurceramsoc.2013.01.030.

[29] V.M. Candelario, F. Guiberteau, R. Moreno, A.L. Ortiz, Aqueous colloidal processing of submicrometric SiC plus Y3Al5O12 with diamond nanoparticles, J. Eur. Ceram. Soc. 33 (2013) 2473–2482. doi:10.1016/j.jeurceramsoc.2013.04.016.

[30] P. Carpio, R. Moreno, A. Gómez, M.D. Salvador, E. Sánchez, Role of suspension

preparation in the spray drying process to obtain nano/submicrostructured YSZ powders for atmospheric plasma spraying, J. Eur. Ceram. Soc. 35 (2015) 237–247. doi:10.1016/j.jeurceramsoc.2014.08.008.

[31] M. Vicent, E. Sánchez, G. Mallol, R. Moreno, Study of colloidal behaviour and rheology of Al2O 3-TiO2 nanosuspensions to obtain free-flowing spray-dried granules for atmospheric plasma spraying, Ceram. Int. 39 (2013) 8103–8111. doi:10.1016/j.ceramint.2013.03.083.

[32] P. Carpio, E. Bannier, M.D. Salvador, A. Borrell, R. Moreno, E. Sánchez, Effect of particle size distribution of suspension feedstock on the microstructure and mechanical properties of suspension plasma spraying YSZ coatings, Surf. Coatings Technol. 268 (2015) 293–297. doi:10.1016/j.surfcoat.2014.08.063.

[33] P. Sokolowski, S. Kozerski, L. Pawlowski, A. Ambroziak, The key process parameters influencing formation of columnar microstructure in suspension plasma sprayed zirconia coatings, Surf. Coatings Technol. 260 (2014) 97–106. doi:10.1016/j.surfcoat.2014.08.078.

[34] R. Moreno, Reología de suspensiones cerámicas, Consejo Superior de Investigaciones Científicas, Madrid, 2005.

[35] P. Carpio, M.D. Salvador, A. Borrell, E. Sánchez, R. Moreno, Alumina-zirconia coatings obtained by suspension plasma spraying from highly concentrated aqueous suspensions, Surf. Coatings Technol. 307 (2016) 713–719. doi:10.1016/j.surfcoat.2016.09.060.

[36] Y. Lin, L. Chen, Oxidation of SiC powders in SiC / alumina / zirconia compacts, Ceram. Int. 26 (2000) 593–598. doi:10.1016/S0272-8842(99)00102-9.